Assembly and Packing of Clathrin into Coats

R. A. CROWTHER and B. M. F. PEARSE
Medical Research Council, Laboratory of Molecular Biology, Cambridge CB2 2QH, England

ABSTRACT We present a model for the packing of clathrin molecules into the characteristic hexagons and pentagons covering coated pits and vesicles. The assembly unit is a symmetrical trimer with three extended legs. Polymerization of these units occurs in seconds under suitable conditions, giving empty polyhedral cages resembling the structures around coated vesicles. Images of small, negatively stained fragments of cages, assembled directly on electron microscope grids, reveal details of the structure, which correlate well with the predicted features of the model.

There is one clathrin trimer at each polyhedral vertex, and each leg of the trimer extends along two neighboring polyhedral edges. Quasi-equivalent packing in pentagons and hexagons in polyhedra of different sizes requires a variable joint at the vertex of the molecule and a hinge in each leg. The construction of clathrin coats is remarkable for the extended fibrous contacts that each molecule makes with many others. Such contacts may confer mechanical strength combined with flexibility needed when a vesicle is pinched off from the membrane.

Coated pits and coated vesicles are ubiquitous structures in the cytoplasm of most eucaryotic cells. Newly forming coated vesicles appear to act as molecular filters in the process of transport between the different membranous organelles of cells (1). They concentrate certain molecules for transfer, while excluding others characteristic of the parent membrane.

Coated membrane is recognized by the remarkable protein lattice present on the cytoplasmic surface of the membrane. The hexagonal and pentagonal features of this lattice were first described by Kanaseki and Kadota (2), who negatively stained coated vesicles in brain extracts. Later, we, together with J. T. Finch (3), determined the basic features of the geometry of the polymorphic range of polyhedral coats seen in purified coated vesicle preparations. Essentially, the coats of vesicles are constructed of 12 pentagonal units plus a variable number of hexagonal units. Coats of greater diameter contain larger numbers of hexagons. More recently, Heuser (4), by rapid-freezing and deep-etching, produced spectacular images of the hexagonal nets on the cytoplasmic surfaces of coated pits on fibroblast plasma membranes. He also showed stages during the formation of coated vesicles, when pentagons are inserted into the lattice.

Clathrin is the major structural protein of the coats (5). It constitutes ~0.5–1% of the protein in postmitochondrial extracts of many cells and tissues, enough to make several thousand coated pits and vesicles per cell (6). It may be purified as a soluble protein by a number of different procedures (7–10). Many of these have in common an extraction step to dissociate the lattice and release the clathrin from the membrane, followed by gel filtration to purify the protein. The resulting preparations generally contain trimers of clathrin, the 180,000-dalton polypeptide, in association with 3 light chains of ~35,000 mol wt, the latter apparently exhibiting some size heterogeneity (7, 11, 12). Such preparations of clathrin trimers have been repolymerized in varying ionic conditions (8–13) to give empty cages resembling the outer coats of coated vesicles. (We propose to use the word "cage" to denote empty shells assembled from purified clathrin, whereas "coat" denotes the complete structure surrounding a vesicle and probably containing additional components besides the clathrin.) Optimal polymerization apparently occurs between pH 6.0 and pH 6.5 in the presence of Ca^{++} or Mg^{++} ions.

Ungewickell and Branton (11) have recently produced shadowed preparations of clathrin trimers and revealed their unusual shape. The trimer consists of three thin legs radiating symmetrically from a central vertex, for which they proposed the name triskelion. We were intrigued how such units could pack to form the characteristic structures of coated pits and vesicles. By investigation of the polymerization of trimers to cages, we have found conditions under which small fragments of cages can be formed on electron microscope grids. Negatively stained preparations of such fragments, photographed with low electron doses, provide clear images, from which the triskelion packing can be elucidated.

MATERIALS AND METHODS

Preparation of Clathrin Trimers

Human placentas were obtained at term from the Maternity Hospital, Mill Road, Cambridge. Crude coated vesicles were separated from placental homogenates essentially as described previously (5, 7) but using a buffer containing 10 mM HEPES, pH 7.2, plus 0.15 M NaCl, 1 mM EGTA, 0.5 mM $MgCl_2$, 0.02%

THE JOURNAL OF CELL BIOLOGY · VOLUME 91 DECEMBER 1981 790–797

sodium azide, and 0.1 mM PMSF (phenylmethylsulfonyl fluoride). An additional step was introduced—namely a 30-min digestion with pancreatic RNase at room temperature to remove ribosomal material before the coated vesicles were pelleted. Clathrin trimers were prepared from such partially purified coated vesicles by a modification of the method of Schook et al. (9). 1 mM PMSF and 1 μg/ml pepstatin were included in buffers throughout. The coated vesicles were diluted eightfold in buffer C (0.02 M Tris-Cl, pH 7.5, 1 mM EDTA, 0.02% sodium azide, and 0.1% β-mercaptoethanol). The suspension was centrifuged at 100,000 *g* for 1 h to remove membranous debris. The remaining supernatant was made 30% saturated in ammonium sulfate at 0°–4°C. The resulting precipitate was collected by centrifugation at 40,000 *g* for 30 min. It was redissolved in the minimum volume of buffer C and dialyzed first against 50 vol of buffer C and then against 2 × 50 vol of buffer D (0.02 M Tris-Cl, pH 7.5, 2 M urea, 1 mM EDTA, 0.1% β-mercaptoethanol, and 0.02% sodium azide). The sample was then applied to a gel filtration column (1 × 150 cm), containing Bio-Gel A15M resin (Bio-Rad Laboratories, Inc., Richmond, Calif.) equilibrated in buffer D. The fractions containing clathrin plus a stoichiometric doublet of low molecular weight polypeptides (of ~32,000 daltons) observed previously (7) were pooled and concentrated by just precipitating the proteins at ~22% ammonium sulfate saturation. The precipitate was collected by centrifugation at 100,000 *g* for 1 h and redissolved in a small volume of buffer D. The solution was dialyzed against 50 vol of buffer D to remove the ammonium sulfate and then against 2 × 50 vol of buffer C to remove the urea.

Sometimes clathrin trimers were obtained by dissolving purified coated vesicles in buffer D, centrifuging at 100,000 *g* for 1 h, and passing the supernatant dialyzed against buffer D over the Bio-Gel A15M column as just described.

Before use in the ensuing experiments, the clathrin trimers were subjected to a cycle of repolymerization and depolymerization as follows:

(*a*) Centrifuge sample in buffer C at 100,000 *g* for 1 h.

(*b*) Dialyze against repolymerization buffer (0.1 M MES [2-(N-morpholino) ethane sulphonic acid] pH 6.5, 1.5 mM $MgCl_2$, 0.2 mM EDTA) (11) for 1 h at room temperature.

(*c*) Centrifuge at 100,000 *g* for 1 h to pellet the reconstituted cages.

(*d*) Resuspend in buffer C and dialyze against buffer C to depolymerize the structures.

(*e*) Centrifuge again at 100,000 *g* for 1 h to give clear supernatant containing clathrin trimers. The purity of the samples was monitored using SDS polyacrylamide gel electrophoresis (14).

Assembly of Clathrin Triskelions to Cages

The efficiency of assembly of the isolated trimers in suitable polymerizing conditions was tested. A solution of clathrin trimers of ~1.0 mg/ml was dialyzed against buffer C′ (buffer C diluted fivefold) to reduce the buffering capacity and the EDTA concentration of the sample. A series of test solutions was set up containing increasing concentrations of trimers between 0 and 1.0 mg/ml. Their absorbances at 280 and 320 nm were measured, using buffer C′ as standard. The ionic conditions of all the samples were then changed to promote polymerization of the triskelions to cages, by the addition to each test tube of 0.1 vol of 1 M MES, pH 6.2, containing 20 mM $MgCl_2$. The optical densities at 320 nm, which after subtraction of the background are proportional to the concentrations of the assembled cages, were then read. Test solutions were monitored in the electron microscope to check that the assembly was into cages and not other aggregates. Finally, the polymerized solutions were centrifuged at 100,000 *g* for 1 h to remove the assembled cages, and the absorbance at 280 nm of the supernatant was measured to give an estimate of the concentration of free triskelions remaining.

Assembly of Fragments of Cages on Electron Microscope Grids

The results of assembly experiments led us to attempt to trap fragments of cages on electron microscope grids. Normally, if an equilibrium exists between free triskelions and cages, one would not expect to see such fragments in solution. In fact, if a grid is made of a polymerizing solution of clathrin, the bulk of the material is in either the cage or the trimer form. However, if a grid is placed on a drop of a solution of triskelions, which are then induced to polymerize, some of the newly forming cage fragments will be made at the grid surface, where it is impossible to add further trimers from the grid side to close the polyhedra.

The procedure we adopted was as follows: A 10-μl drop of triskelions at 0.2 mg/ml (where ~75% should polymerize) in buffer C′ was placed on a square of parafilm, and an electron microscope grid was put face down on the surface of the droplet. 1 μl of 1 M MES buffer, pH 6.0, was injected into the solution to induce polymerization. In the resulting ionic conditions (0.1 M MES, pH 6.0, with no Mg^{++}), the polymerization is much slower than in the presence of magnesium. After leaving for 3 min to allow cage fragments to form, the grid was removed and stained. If a second grid was then applied to the droplet, completed cages made in solution were observed rather than the fragments, trapped during assembly, that were seen on the first grid.

Electron Microscopy

Specimens were deposited or assembled on a thin carbon film supported by a thicker carbon film with holes. Negative staining was produced by washing with a few drops of 1% aqueous uranyl acetate, leaving for a few seconds, and then drawing off the excess liquid with a piece of filter paper. Specimens were examined in a Philips EM301 electron microscope using an accelerating voltage of 80 kV, and pictures were taken on Kodak electron image film at a nominal magnification of × 45,000. Calibration of the magnification was carried out by mixing clathrin specimens with T4 phage and using the clear 41-Å stripe on the phage tail (15) as a reference. Pictures were taken at 4,000–5,000 Å underfocus sufficient to give good phase contrast in the images without introducing spurious features (16). Low electron doses (17) were used to minimize the beam damage to the specimen. The technique used was to focus on an area of specimen, cut off the beam by moving the C1 condenser aperture a pre-set amount (18), move the specimen by a small amount to give an unexposed area, and then make an exposure manually using the C1 aperture as a shutter.

Rotational filtering (19) was used to improve the signal-to-noise ratio in images of threefold symmetric vertices in small fragments of cages. In this technique the densitometered image is analyzed by computer into a series of angularly varying functions, whose relative strengths can be estimated. The degree of symmetry of the image and thus the preservation of the specimen can therefore be quantitatively assessed and the best images chosen. A rotationally filtered image is then produced by numerically summing just those angularly varying functions consistent with the symmetry of the specimen, which in this case is threefold.

RESULTS

Polymerization of Triskelions to Cages

Triskelions in Buffer C′ were polymerized from solutions of different protein concentration by the addition of 0.1 vol of 1 M MES buffer, pH 6.2, containing 20 mM $MgCl_2$. In the resulting ionic conditions, polymerization occurred within seconds. After subtraction of small background absorbances, the optical densities at 320 nm of the final solutions are attributable to light scattering by assembled cages and are proportional to cage protein concentration. These optical densities were plotted against the initial total protein concentrations, measured by absorbance at 280 nm. A typical set of results is shown in Fig. 1. At total protein concentrations of <0.05 mg/ml, no polymerization was observed, whereas above this value the extent of polymerization increased linearly with the total protein concentration. The remaining supernatant protein, after polymerized material had been removed by centrifugation, contained free triskelions at a nearly constant concentration of ~0.05 mg/ml. This suggests that clathrin assembly in vitro has the properties of an equilibrium association, and that above a critical concentration of triskelions self-association into cages occurs (20).

Images of Individual Clathrin Molecules

Ungewickell and Branton (11) visualized individual molecules of clathrin, by heavy metal shadowing and less clearly by negative staining, as extended triskelion-like structures. Using low electron doses, we have produced clear images showing similar structures in negatively stained preparations of disaggregated clathrin coats (Fig. 2). The legs look rather more slender (~30–40 Å thick) in our negatively stained preparation than in the shadowed preparation of Ungewickell and Branton (11) and do not appear to show the knob at the tip. This difference could well arise from the buildup of metal during shadowing, which would tend to exaggerate the thickness. The arc length of the leg, from the center of the threefold vertex to the apparent tip of the leg, was measured by making × 9

photographic enlargements of the micrographs, drawing over the legs with a fine pen, and then measuring the resulting arcs with a computer-linked graphics tablet, using an arc-integrating program written by Dr. T. S. Horsnell. The average leg length was 433 ± 43 Å (96 legs measured), in good agreement with the value of 445 ± 23 Å obtained by Ungewickell and Branton (11). The larger standard deviation in our measurements arises from the greater uncertainty in defining the tip of the leg in negatively stained preparations than in shadowed ones.

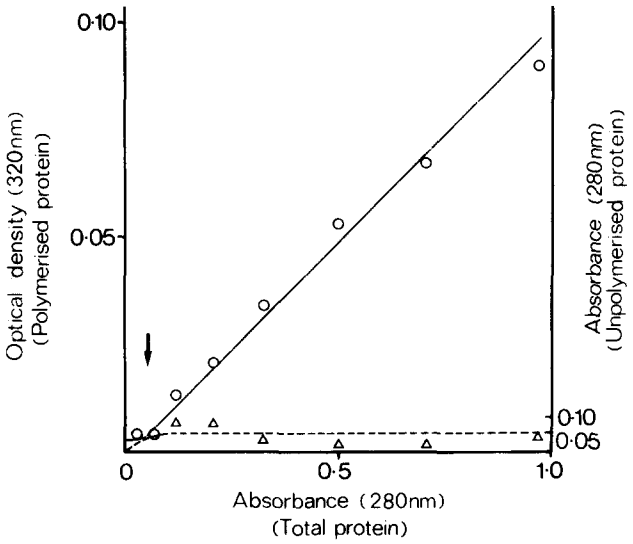

FIGURE 1 Polymerization of triskelions to form cages. Triskelions were polymerized from solutions of increasing total protein concentration, measured spectrophotometrically by the initial absorbance at 280 nm (abscissa). The amount of assembly in each solution was monitored by reading the optical density at 320 nm (○; left-hand ordinate). Assembled cages were then removed by centrifugation at 100,000 *g* for 1 h and the concentration of free triskelions was measured by the absorbance at 280 nm (△; right-hand ordinate).

The contour shape of the leg varies from fairly uniformly curved to quite sharply kinked. Selecting the subpopulation of particles exhibiting a sharp kink near to the vertex, we estimate that the distance from the kink to the vertex is ~160 ± 10 Å (20 legs measured). There is a smaller standard deviation in this measurement than in that of the whole leg as we chose sharp kinks, which were better defined than the tips of the legs. This estimate is smaller than the 189 ± 12 Å reported by Ungewickell and Branton for their shadowed preparation.

It is striking that virtually all the triskelions exhibit the same handedness, implying that the clathrin must have a preferred side of attachment to the carbon film. In our convention of printing, this view with the legs curving round anticlockwise corresponds to viewing the molecule from the side attached to the carbon film.

Partly Reassembled Cages

In negatively stained preparations of reassembled clathrin, one occasionally sees images that represent either partly completed cages or possibly one-sided images arising from partial embedding of the cage in the stain. Such images (Fig. 3) provide a particularly clear view of the local polygonal structure of the cage and allow an accurate measurement of the polygonal edge length. Measurement of the negatives directly with a Nikon microcomparator, using T4 phage tails as a

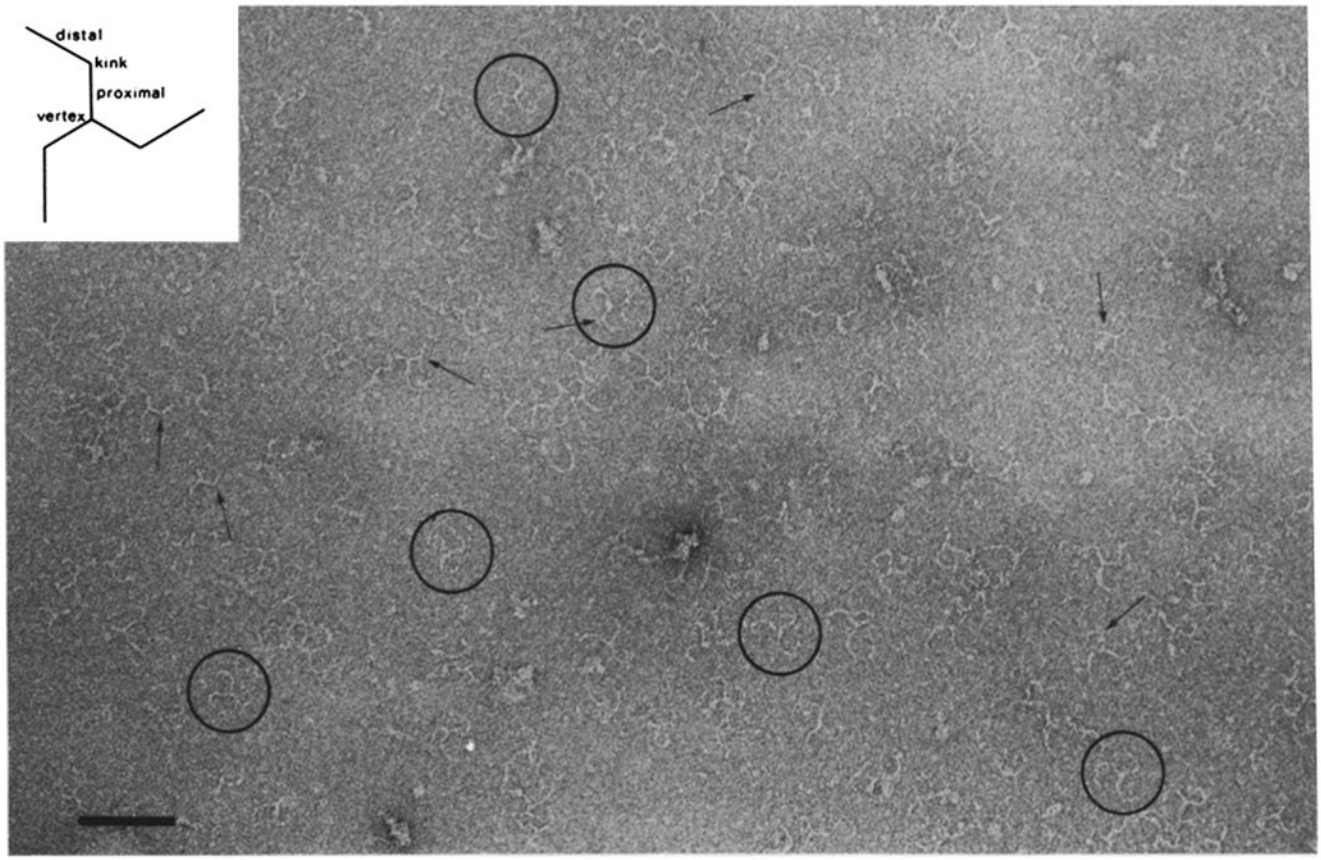

FIGURE 2 Individual clathrin triskelions, negatively stained with uranyl acetate. A few examples have been ringed and others can be seen in the field. The arrows indicate examples of sharp kinks in the legs, occurring at ~160 Å from the vertex of the triskelion. Bar, 1,000 Å. × 126,000. *Inset:* diagram of a triskelion showing the names used in the text to denote the various parts.

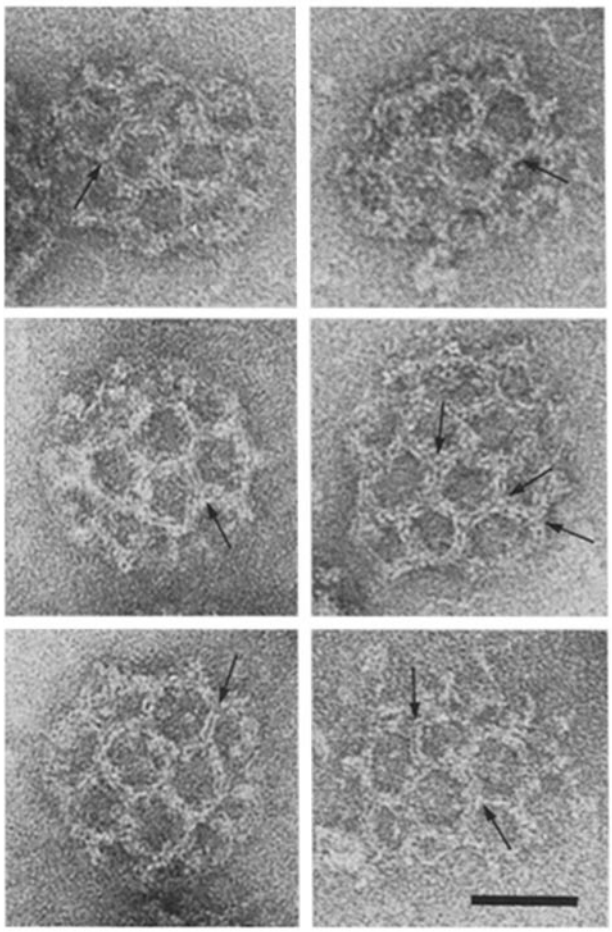

FIGURE 3 Large fragments of clathrin cages, negatively stained with uranyl acetate. Some edges exhibiting a clear double or triple lined nature are indicated by arrows. Bar, 500 Å. × 280,000.

standard, gave a value of 186 ± 7 Å (52 edges measured) for the distance between neighboring threefold vertices, measured from center of vertex to center of vertex. This is larger than our previous estimate (3) of 150 Å, which we obtained from coated vesicles embedded in broken stain films and therefore expected to be shrunken.

The other observation to be made from these images is that the polygonal edges of the cage sometimes appear split longitudinally into two clear lines or three less clear lines of stain-excluding material (indicated by arrows in Fig. 3). The separation between the lines of density is ~30–40 Å. When an edge appears triple the central line of density frequently appears heavier than the two flanking lines and appears to stop short of the vertex. (This effect is seen most clearly when the image is viewed obliquely along the direction of the edge.) Besides the appearance of these tram lines of density radiating from the vertex, there is sometimes a dot of stain excluding material actually on the threefold position.

Some Packing Models

At this stage, it is necessary to introduce some possible models for the packing of triskelions in larger assemblies, so that the features seen in the images can be interpreted and further clues sought to allow the various models to be distinguished. Granted the three-coordinated nature of the polygonal structures of small coats (3) and of larger arrays seen in freeze-fractured cells (4), it is natural to place the vertex of the triskelion at the vertex of the polygonal coat. Because the clathrin trimer forms pentagons and hexagons (2–4) and also heptagons (4), there must be a triskelion at every vertex in a completed structure. One could form a hexagon from three triskelions placed at alternate vertices, but this arrangement would not generalize to allow formation of pentagons and heptagons (12). Provided there is a triskelion at each vertex, a pentagon or heptagon can be formed from a hexagon by removing or adding a triskelion, which could be accommodated with only small distortions of the molecule, in the same way that a protein subunit packs quasi-equivalently to make groups of five or six molecules in a virus capsid (21).

The length of leg of the triskelion is such that it could run along two neighboring polygonal edges or possibly fold back sharply on itself to run twice along a given edge. The latter possibility seems unlikely as we do not see the legs of individual triskelions folded back sharply on themselves, nor do the polygonal structures have the appearance that this type of packing would confer. In individual triskelions the kink in the leg is ~160 Å from the vertex, so that the distal part of the leg must veer off before reaching the neighboring vertex 186 Å away. Two types of packing are then possible, either a simple side-by-side type of packing (Fig. 4*a*) or a more complicated packing involving a cross-over (Fig. 4*b*), according to the orientation of the triskelion within the polyhedral lattice. The appearance of the resulting polyhedral vertex is very different in the two cases and we believe that features in the images favor the cross-over type of model. In Fig. 4*c*, we show a pentagon with the cross-over packing to emphasize that it can be formed in the same way as a hexagon, with only small distortions of the molecules.

With the packings shown diagrammatically in Fig. 5, each edge of a completed polyhedron will be formed by the proximal halves of two legs running from neighboring vertices and the distal halves of two legs running from vertices one step farther away on the polyhedral lattice. The whole arrangement will have a local twofold axis of symmetry midway between the threefold vertices and normal to the edge. The appearance of such an edge seen by negative staining will depend on how the four half-legs associate with one another and how the stain penetrates between them. If each distal half associates closely with a proximal half, a double-lined appearance will result (Fig. 5*a*). If, however, the two proximal halves are strongly associated while the distal halves are more loosely associated, a triple-lined pattern results (Fig. 5*b*), with the central line appearing heavier than the outer two. Both these patterns are seen in the partly completed coats (Fig. 3), suggesting some variability of structure or staining.

The cross-over packing with a double edge (Fig. 5*a*) gives rise to a particularly striking pattern around the vertex, consisting of an equilateral triangle orientated such that one vertex of the triangle points roughly at right angles to the polyhedral edge. There is a dot in the middle of the triangle corresponding to the material at the vertex of an individual triskelion. Note also that the doublet line is skewed clockwise by ~6° with respect to an (imaginary) line joining the threefold vertices, since in the cross-over packing individual triskelions are rotated clockwise from a position in which each leg points directly at a neighboring vertex. One line of each doublet is colinear with an edge of the equilateral triangle described about the vertex and the double lines appear to radiate from the triangle in a maximally skewed manner. Thus at a vertex, in the orientation of Fig. 5*a*, the two sloping edges appear to join the vertical

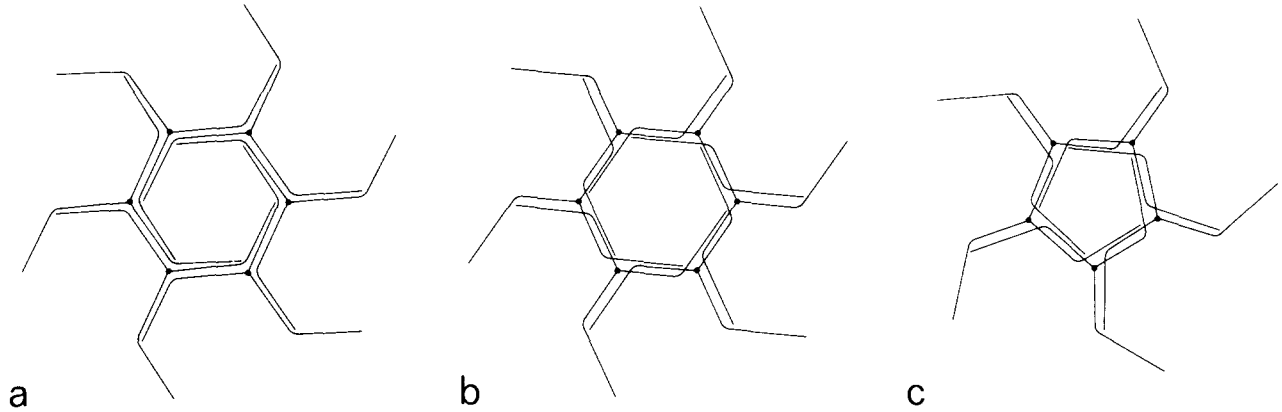

FIGURE 4 Some models for the packing of triskelions. In each case there is a triskelion at every vertex of the polygon and each leg of the triskelion runs along two adjacent polygonal edges. (*a*) A hexamer of triskelions with simple side-by-side packing of the legs. (*b*) A hexamer of triskelions with a cross-over packing of the legs. (*c*) A pentamer of triskelions, showing that this can be constructed in the same way as the hexamer (*b*), with only small distortions of the triskelion.

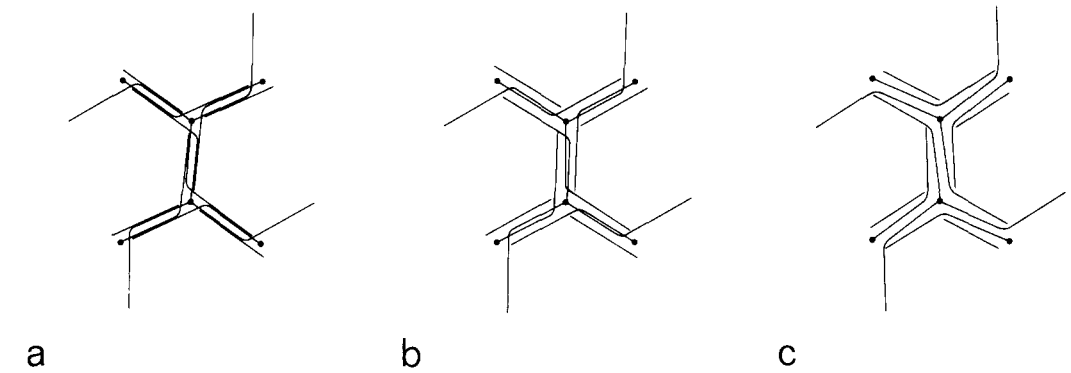

FIGURE 5 The appearance of a polyhedral edge in various packing models. Each diagram shows two complete triskelions at neighboring polyhedral vertices, together with the parts of more distant triskelions that contribute to these two vertices and the adjoining polyhedral edges. Each edge consists of two proximal half-legs and two distal half-legs. In *a*, the cross-over packing is shown with the proximal half-leg closely associated with the adjacent distal half-leg to produce an apparently double line along the edge. *b* also shows the cross-over packing but with the two proximal half-legs closely associated and the distal halves more loosely associated, giving the edge a triple-lined appearance. Such double- and triple-lined edges are seen in the coats shown in Fig. 3. *c* shows the side-by-side packing, which gives rise to vertices and edges quite different in appearance from the cross-over packing shown in *a* and *b*.

edge in a staggered disposition and the polygonal holes (pentagons or hexagons) therefore appear rotated relative to the underlying lattice (see also Fig. 7*d*). In the corresponding side-by-side packing (Fig. 5*c*), the pattern around the vertex does not have the striking triangular appearance and the double line is skewed anticlockwise, corresponding to an anticlockwise rotation of the triskelion, though less markedly than in the cross-over packing. The stagger of edges joining a vertex also appears much less noticeable.

Images of Small Fragments of Cages

To see how the triskelion assembly units pack together to form the completed clathrin cages, one must look at large numbers of small fragments of cages. We found that the best way to do this was to let the clathrin assemble on the grid under conditions of slow assembly (see Materials and Methods). In this way one can trap individual pentagons and hexagons and also larger pieces comprising two or more polygonal faces producing fields such as that shown in Fig. 6*a*.

Individual pentagons and hexagons, shown in Fig. 6*b* and *c* have projections that radiate outward from each vertex and that taken overall give an impression of bending round in an anticlockwise manner, as would be expected for the packings drawn in Fig. 4. Similar projections from vertices of larger aggregates also appear to bend round anticlockwise, if they show any distinct handedness. The proximal parts of the projections, formed by a proximal and a distal half-leg of the triskelion, appear much clearer than the distal parts, which consist of only a distal half-leg of the triskelion. The symmetry of the pentagons and hexagons, which display an equal weighting of all their vertices, implies that there is a triskelion at each vertex, as was argued above on the basis of quasi-equivalent packing in pentagons, hexagons, and heptagons. (We have not seen any individual heptagons in our experiments, suggesting that this is a more strained configuration than the pentagon or hexagon, which appear in roughly equal numbers.)

The side-by-side packing (Figs. 4*a* and 5*c*) and the cross-over packing (Figs. 4*b* and 5*a*) may be distinguished by examining the appearance of individual edges and vertices, such as those shown in Fig. 7*a*. These all show features characteristic of the cross-over packing (Figs. 5*a* and 7*b*), the most striking example being indicated by an asterisk in Fig. 7*a*. The characteristic features are that the distribution of protein around the vertex of the polygon has a triangular appearance, while the matter forming the edge of the polygon

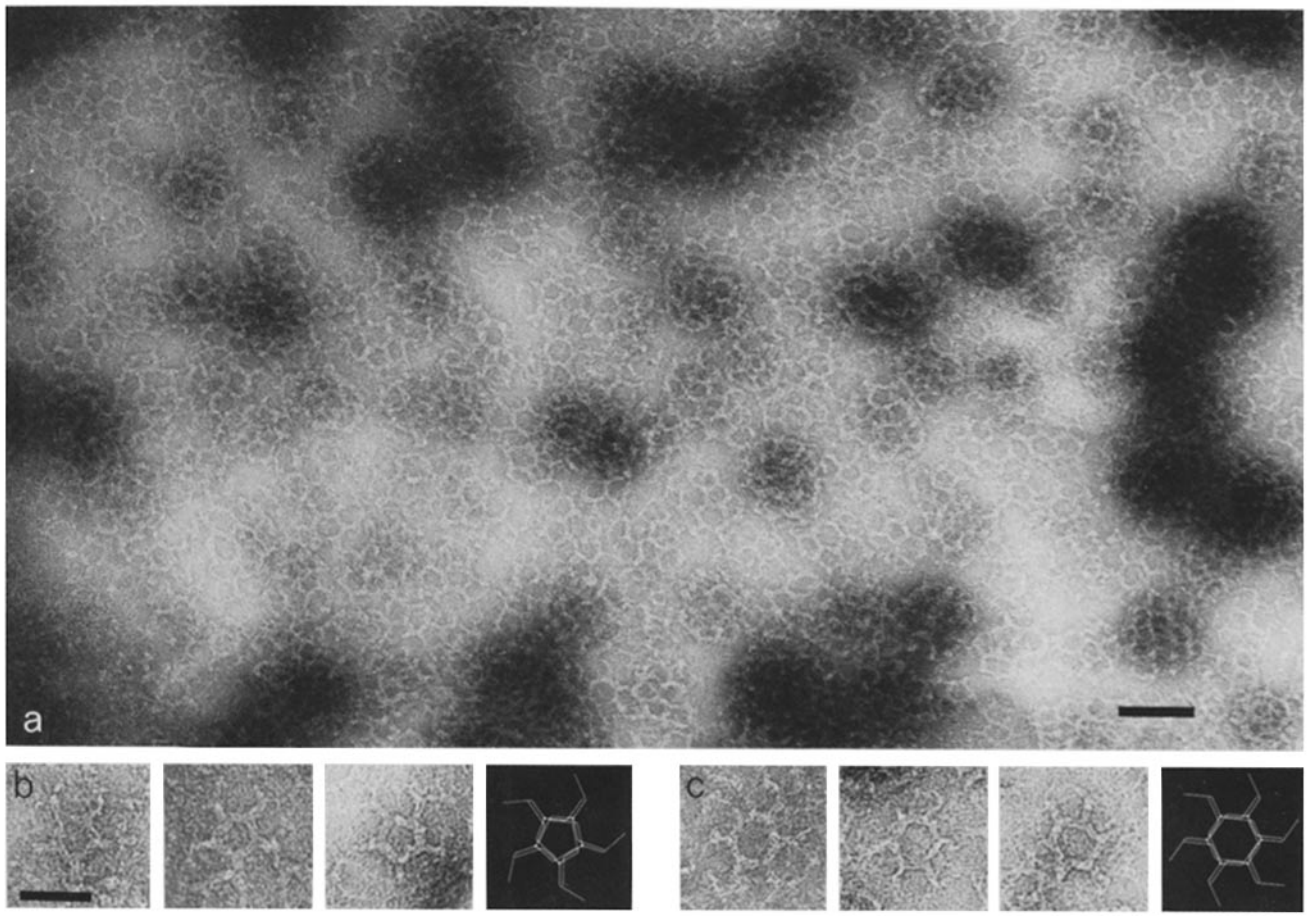

FIGURE 6 Small fragments of cages trapped on the microscope grid during assembly. (*a*) A general field. Bar, 1,000 Å. × 105,000. (*b*) Individual pentagons compared with the model in Fig. 4 *b*. (*c*) Individual hexagons compared with the model in Fig. 4 *c*. (*b* and *c*) Bar, 500 Å. × 195,000.

appears skewed clockwise relative to the line joining the threefold positions. The skewed arrangement may be perceived locally in the structure of an individual vertex or globally in the disposition of three neighboring polygons. This is demonstrated more clearly in Fig. 7 *c* by the threefold rotationally filtered image of a vertex, showing that the three polygonal edges join the vertex in a staggered manner. Alternatively, Fig. 7 *d* shows diagrammatically that the hexagonal or pentagonal holes in the lattice, with sharp corners formed by a distal half-leg crossing a proximal one, appear rotated clockwise relative to the underlying lattice, so that an edge is not perpendicular to the line joining the centers of the two polygons on either side of that edge. These features are exactly the ones expected for the cross-over packing, which has been superimposed as dotted lines on the filtered image (Fig. 7 *c*). It does not look at all like the pattern produced by side-by-side packing (Fig. 5 *c*). The cross-over packing shown in Fig. 5 *a* accounts for ~350 Å of the leg of the triskelion, so there must be an additional ~80 Å at the distal tip not included in the model. It is not possible to tell from the present pictures what the conformation of this distal tip might be.

DISCUSSION

A remarkable feature of clathrin polymerization at pH 6.2 and 2 mM Mg^{++} is the speed at which it occurs—it is complete in seconds. The assembly behaves like a condensation process (20), where, above a critical protein concentration, clathrin trimers self-associate to form cages, in equilibrium with a constant low concentration of monomer triskelions. This type of assembly mechanism is typical of many protein aggregates, e.g., actin and tobacco mosaic virus (22).

In the cell, clathrin triskelions probably add on to already existing rafts of hexagonal clathrin lattice apposed to the cytoplasmic surface of a membrane. In vivo, a high proportion of the total clathrin (~0.05 mg/ml of cytoplasm) is in the form of coats on membranes. Thus, the concentration of free triskelions in solution is likely to be much lower than the critical protein concentration (~0.05 mg/ml) that we estimate in near optimal polymerization conditions for isolated clathrin. However, at pH 7.0 and above, the empty clathrin cages rapidly fall apart. Therefore, in a cycle of coated vesicle function, the fine control of clathrin assembly and dissociation must depend on other factors, probably including other proteins found in coated vesicles (e.g., those of 100,000 mol wt).

The basic cage structure is formed from one clathrin triskelion at each polyhedral three-coordinated vertex, with each leg extending along two neighboring polyhedral edges. Each polyhedral edge thus consists of the proximal parts of two legs and the distal parts of two other legs. The packing that we propose for triskelions involves a small clockwise rotation of the triskelion relative to the underlying polyhedral lattice, so that the legs of the triskelion do not point directly at the neighboring vertices but slightly to one side. Coupled with an anticlockwise kinking of each leg, this implies a cross-over type of packing, producing the characteristic features in individual

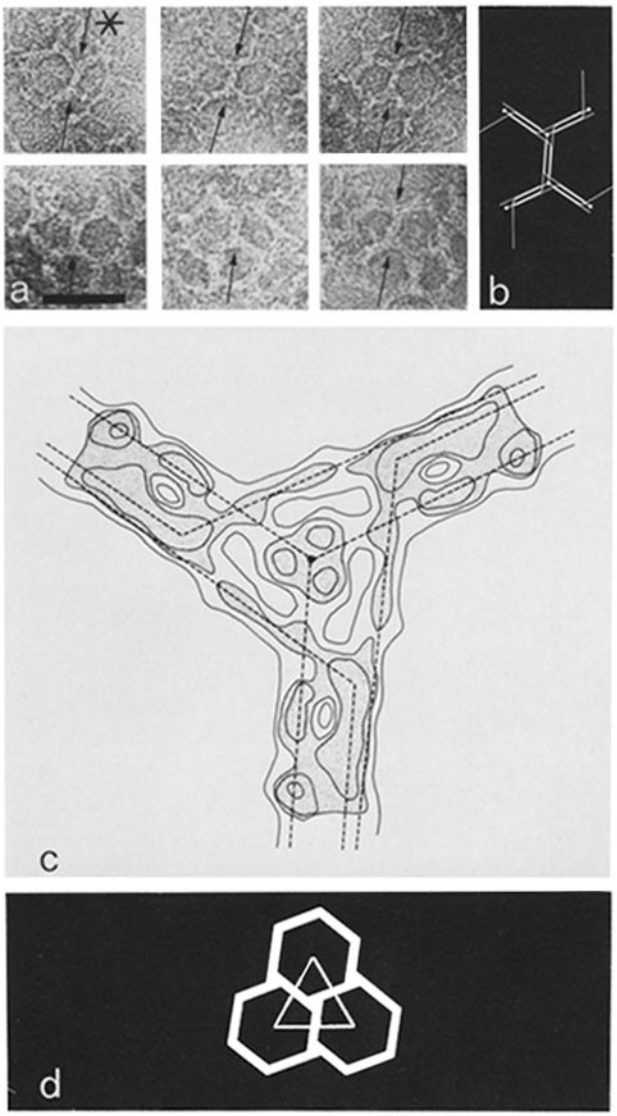

FIGURE 7 The appearance of individual edges and vertices. (*a*) Electron micrographs of small fragments of cages, with characteristic edges or vertices indicated by arrows. Bar, 500 Å. × 215,000. (*b*) Model for edge based on the cross-over packing shown in Fig. 5 *a*. Note the similarity between this model and the images in *a* (see text). (*c*) A threefold rotationally filtered image, produced using computer programs described by Crowther and Amos (19), of the upper vertex (*) in the first micrograph of the series. The image is presented as a contour map with the stippled areas representing stain-excluding material. The dotted lines superimposed on the map show the geometry of triskelion legs expected in the cross-over packing model, which can be seen to agree well with observed distribution of stain-excluding material. (The three legs whose distal halves terminate near the vertex have been omitted for clarity, though there appears to be sufficient density to accommodate them.) (*d*) Diagrammatic representation of three neighboring hexagons, in which the skewing has been slightly exaggerated, to show that an edge is not perpendicular to the line joining the centers of the two polygons on either side of that edge.

vertices and edges described above. Our pictures are printed to show the structures from the side attached to the carbon film on the electron microscope grid. If it is the vesicle side of the clathrin that is bound to the carbon film, as suggested by the limited growth of fragments of cages bound to the grid, our convention corresponds to viewing the triskelion and the corresponding fragments from the inside of the cage. However, this suggestion still requires proof.

Although the molecular packing in the cages is governed by the general principles of quasi-equivalence first suggested for viral capsids (21), the realization of the design is very different. In the virus structures studied so far, the capsid proteins are relatively compact and the domains of interaction between the subunits relatively localized (23). By contrast, the clathrin triskelion is a highly extended fibrous molecule which, when it packs to form cages, interacts extensively not only with its nearest neighbors but also with quite distant molecules. In this respect the packing of clathrin resembles that of fibrous muscle proteins, such as myosin and tropomyosin, which make extended contacts between themselves and with other muscle proteins in fibrillar aggregates. The remarkable thing about clathrin is that it uses similar extended fibrous contacts to produce isometric shells with a high degree of specificity. This specificity implies that the clathrin molecule must be a relatively stiff structure, though containing a variable joint at the vertex of the triskelion and a hinge in the leg at ~160 Å from the vertex. The former permits the variation in the conical angle at the vertex needed in forming aggregates varying from almost planar (4) to quite sharply curved (3). The latter is needed to accommodate the extended leg to the difference in angle between neighboring edges in pentagons and hexagons. Such a molecular design, coupled with the extended nature of the packing contacts, allows formation of shells with a wide range of curvatures, while maintaining the specificity of construction and conferring the mechanical strength combined with flexibility needed when a vesicle is pinched off from the membrane.

We thank Drs. Ungewickell and Branton for sending us a preprint of their paper. We are grateful to our colleagues, Drs. Finch, Kilmartin, Bretscher, and Klug, for their helpful comments on the manuscript.

B. M. F. Pearse is supported by a research fellowship from the Science Research Council.

Received for publication 29 April 1981, and in revised form 23 July 1981.

REFERENCES

1. Bretscher, M. S., J. Nichol Thomson, and B. M. F. Pearse. 1980. Coated pits act as molecular filters. *Proc. Natl. Acad. Sci. U. S. A.* 77:4156–4159.
2. Kanaseki, T., and K. Kadota. 1969. The vesicle in a basket. *J. Cell Biol.* 42:202–220.
3. Crowther, R.A., J. T. Finch, and B. M. F. Pearse. 1976. On the structure of coated vesicles. *J. Mol. Biol.* 103:785–798.
4. Heuser, J. 1980. Three dimensional visualization of coated vesicle formation in fibroblasts. *J. Cell Biol.* 84:560–583.
5. Pearse, B. M. F. 1975. Coated vesicles from pig brain: purification and biochemical characterization. *J. Mol. Biol.* 97:93–98.
6. Pearse, B. M. F. 1976. Clathrin: a unique protein associated with intracellular transfer of membrane by coated vesicles. *Proc. Natl. Acad. Sci. U. S. A.* 73:1255–1259.
7. Pearse, B. M. F. 1978. On the structural and functional components of coated vesicles. *J. Mol. Biol.* 126:803–812.
8. Keen, J. H., M. C. Willingham, and I. H. Pastan. 1979. Clathrin-coated vesicles: isolation, dissociation and factor-dependent reassociation of clathrin baskets. *Cell.* 16:303–312.
9. Schook, W., S. Puszkin, W. Bloom, C. Ores, and S. Kochwa. 1979. Mechanochemical properties of brain clathrin. *Proc. Natl. Acad. Sci. U. S. A.* 76:116–120.
10. Nandi, P. K., H. T. Pretorius, R. E. Lippoldt, M. L. Johnson, and H. Edelhoch. 1980. Molecular properties of the reassembled coat protein of coated vesicles. *Biochemistry.* 19: 5917–5921.
11. Ungewickell, E., and D. Branton. 1981. Assembly units of clathrin coats. *Nature (Lond.).* 289:420–422.
12. Kirchhausen, T., and S. C. Harrison. 1981. Protein organization in clathrin trimers. *Cell.* 23:755–761.
13. Woodward, M. P., and T. F. Roth. 1978. Coated vesicles: characterization, selective dissociation and reassembly. *Proc. Natl. Acad. Sci. U. S. A.* 75:4394–4398.
14. Laemmli, U. K. 1970. Cleavage of structural proteins during the assembly of the head of bacteriophage T4. *Nature (Lond.).* 227:680–685.
15. Moody, M. F. 1971. Structure of the T2 bacteriophage tail-core and its relation to the assembly and contraction of the sheath. Proceedings of the First European Biophysics Congress, Baden, Austria. Verlag der Wiener Medizinischen Akademie, Vienna. 543–546.
16. Erickson, H. P., and A. Klug. 1971. Measurement and compensation of defocussing and aberrations by Fourier processing of electron micrographs. *Philos. Trans. R. Soc. Lond. B.*

Biol. Sci. 261:105–118.
17. Williams, R. C., and H. W. Fisher. 1971. Electron microscopy of tobacco mosaic virus under conditions of minimal beam exposure. *J. Mol. Biol.* 52:121–123.
18. Unwin, P. N. T., and R. Henderson. 1975. Molecular structure determination by electron microscopy of unstained crystalline specimens. *J. Mol. Biol.* 94:425–440.
19. Crowther, R. A., and L. A. Amos. 1971. Harmonic analysis of electron microscope images with rotational symmetry. *J. Mol. Biol.* 60:123–130.
20. Oosawa, F., and M. Kasai. 1962. A theory of linear and helical aggregations of macromolecules. *J. Mol. Biol.* 4:10–21.
21. Caspar, D. L. D., and A. Klug. 1962. Physical principles in the construction of regular viruses. *Cold Spring Harbor Symp. Quant. Biol.* 27:1–24.
22. Oosawa, F., and S. Asakura. 1975. Thermodynamics of the Polymerization of Protein. Academic Press, London. 25–40.
23. Harrison, S. C. 1980. Virus crystallography comes of age. *Nature (Lond.).* 286:558–559.